

Technical Report Documentation Page

1. Report No.	2. Government Accession No.	3. Recipient's Catalog No.	
4. Title and Subtitle		5. Report Date	
		6. Performing Organization Code	
7. Author(s)		8. Performing Organization Report No.	
9. Performing Organization Name and Address		10. Work Unit No. (TRAIS)	
		11. Contract or Grant No.	
12. Sponsoring Agency Name and Address		13. Type of Report and Period Covered	
		14. Sponsoring Agency Code	
15. Supplementary Notes			
16. Abstract			
17. Key Words		18. Distribution Statement	
19. Security Classif. (of this report) Unclassified	20. Security Classif. (of this page) Unclassified	21. No. of Pages	22. Price

Measurements of Nitrile Rubber Absorption of Hydrocarbons: Trends for Sustainable Aviation Fuel Compatibility

Conor Faulhaber,* Christopher Borland, Randall Boehm, and Joshua Heyne*

Cite This: <https://doi.org/10.1021/acs.energyfuels.3c00781>

Read Online

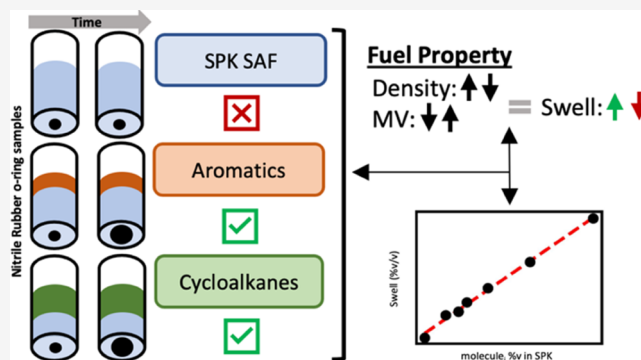
ACCESS |

Metrics & More

Article Recommendations

Supporting Information

ABSTRACT: The commercial aviation sector is seeking to reach net zero CO₂ emissions by 2050, with sustainable aviation fuel (SAF) being the most important lever. However, SAF is currently limited by ASTM specifications to a maximum of 50%v blending with conventional jet fuel. One reason for the current blend limit is motivation to maintain o-ring swelling consistent with 100% petroleum fuel. This work explores the relationships between o-ring swelling of SAF blend components, model compounds, and various blends in nitrile rubber compared to conventional fuel swelling. Specifically, optical dilatometry measurements were used to gather swell propensity data for 39 different hydrocarbon dopants at 8%v in an *iso*-alkane solution, 4 dopants at 7 different concentrations, and 19 different fuels or fuel blends. This study also highlights the advantages of using swell measurements, such as those employed here, as a quality control metric instead of the current 8%v aromatics requirement. Notably, the potential is shown to maintain swelling in the conventional fuel range with fuels composed of less than 8%v aromatics.



1. INTRODUCTION

The U.S. aviation industry as well as the international community has made public its intentions to become a net zero CO₂ emissions industry by 2050.^{1,2} To accomplish this goal, the sustainable aviation fuel (SAF) Grand Challenge was initiated to expand SAF production to 3 billion gallons per year by 2030, and 35 billion gallons per year by 2050.³ SAF derived from renewable feedstocks, like agricultural waste or used cooking oil, has become a particular interest of the industry because of its unique, near-term advantages over other sustainable sources of aircraft propulsive energy: electricity, hydrogen fuel cells, and hydrogen combustion. Namely, SAF is presently the only feasible option for long-haul flights, which are the largest contributor to aircraft emissions,⁴ and offers a high potential for backward compatibility with existing fuel and engine systems. However, until advancements in SAF technologies can guarantee 100%v “drop-in” capability, the specification for fuels containing synthesized hydrocarbons^{5,6} limits SAF to a maximum of 50%v blending with conventional fuel. Resolving the motivating factors behind this blending limit are of high value to the industry as it works toward the stated production targets.

The 50%v cap on SAF blend fractions in jet fuel is set to mitigate the risk introduced by fuel composition variance outside of the experience range with conventional fuels. Coincidentally, this limit currently aligns with the 8%v minimum aromatics requirement and the 775 kg/m³ minimum density requirement.⁵ Despite being associated with higher

nonvolatile particulate matter (nvPM) emissions and, in turn, aviation’s contribution to radiative forcing via contrails,^{7,8} aromatics are currently mandated at a minimum of 8%v in jet fuel largely because they are primarily responsible for elastomer o-ring swelling in fuel systems.^{9,10} Six of the seven currently approved SAF pathways result in hydrocarbon mixtures with low aromatic content (specifically, less than 0.5%v⁵) and low density. Acceptable blends with conventional fuels may contain significantly less than 50%v SAF depending on the density, aromatic content, or some other property of the conventional fuel component, where in situ testing of density (easy) and aromatics content (harder) is required to maximize the fraction of SAF that can be used.

Relatively consistent o-ring swelling is necessary for existing systems to maintain seal connections and prevent fuel leakage, particularly in systems with aged o-rings, which have taken on some level of compression set (loss of elasticity). Though there is little documented operational experience of this issue, one instance of this type of leakage was observed in an initial test of an approved SAF, synthetic paraffinic kerosene (SPK), during

Received: March 8, 2023

Revised: May 24, 2023

Table 1. All Hydrocarbon Dopants Used in This Study with Purity, Vendor, Density, and Structural Information

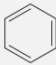
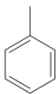
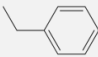
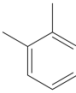
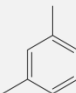
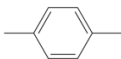
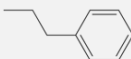
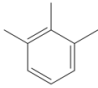
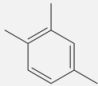
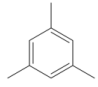
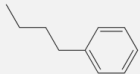
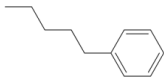
Molecule Name	Purity [%]	Vendor	Density at 15°C [kg/m ³]	Molecule Structure
alkylbenzenes				
benzene	>99.8	Millipore Sigma	884.0	
toluene			869.0	
ethylbenzene	>99.0	Honeywell	871.6	
ortho-xylene	>98.0	TCI America	883.9	
meta-xylene	>99.0	TCI America	868.5	
para-xylene	99	Alfa Aesar	866.7	
<i>n</i> -propylbenzene	>99.0	TCI America	867.0	
1,2,3-trimethylbenzene	>99.0	Sigma Aldrich	897.8	
1,2,4-trimethylbenzene	>98.0	TCI America	879.7	
1,3,5-trimethylbenzene	>97.0	TCI America	869.3	
<i>n</i> -butylbenzene	>99.0	Acros Organics	865.1	
<i>n</i> -pentylbenzene	96	Alfa Aesar	855.8	

Table 1. continued

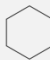
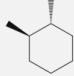
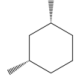
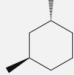
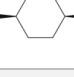

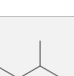
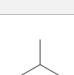





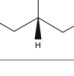
Molecule Name	Purity [%]	Vendor	Density at 15°C [kg/m ³]	Molecule Structure
alkylbenzenes				
<i>n</i> -hexylbenzene	98	Alfa Aesar	863.6	
<i>n</i> -heptylbenzene	>97.0	TCI America	862.1	
cyclo-aromatics				
tetralin	>97.0	TCI America	973.6	
indane	>95.0	TCI America	967.5	
naphthalenes				
1-methylnaphthalene	>98.0	TCI America	1023.8	
2-ethylnaphthalene	>99.0	TCI America	996.8	
2-isopropylnaphthalene	>95.0	TCI America	975.3	
biphenyl				
biphenyl	99	Alfa Aesar	1041.0	
monocycloalkanes				
cyclohexane	>99.0	Fisher Chemical	784.2	
methylcyclohexane	99	Sigma Aldrich	769.4	
ethylcyclohexane	>99.0	Acros Organics	794.2	
<i>cis</i> -1,2-dimethylcyclohexane	>98.0	TCI America	802.4	

Table 1. continued

Molecule Name	Purity [%]	Vendor	Density at 15°C [kg/m ³]	Molecule Structure
monocycloalkanes				
<i>trans</i> -1,2-dimethylcyclohexane	>99.0	TCI America	781.5	
<i>cis</i> -1,3-dimethylcyclohexane	>99.0	TCI America	773.0	
<i>trans</i> -1,3-dimethylcyclohexane	>95.0	TCI America	789.4	
<i>cis</i> -1,4-dimethylcyclohexane	>98.0	TCI America	788.5	
<i>trans</i> -1,4-dimethylcyclohexane	>95.0	TCI America	768.8	
<i>n</i> -propylcyclohexane	>98.0	TCI America	793.8	
1,2,4-trimethylcyclohexane	>96.0	TCI America	785.8	
1,3,5-trimethylcyclohexane	>98.0	TCI America	778.9	
<i>n</i> -butylcyclohexane	99	Alfa Aesar	804.0	
<i>n</i> -pentylcyclohexane	98	Alfa Aesar	807.0	
<i>n</i> -hexylcyclohexane	>98.0	TCI America	812.0	
<i>n</i> -heptylcyclohexane	>99.0	TCI America	805.3	
polycycloalkanes				
<i>cis</i> -decalin	>98.0	TCI America	900.7	

a test campaign at NASA Glenn.¹¹ This issue can be compounded by the effects of fuel cycling over the lifetime

of an o-ring. As reported at Kelly AFB in 1983, when an aircraft is refueled or when the fuel system is emptied during

downtime, it is possible for an o-ring to swell or shrink depending on the level of aromatics it is exposed to.¹² Intermittent swell and relaxation of the o-ring caused by variations in fuel composition may adversely affect the material strength of the elastomer over time.¹³ Though the Kelly AFB example does not directly deal with SAF, its emphasis on the consistency of swelling behavior with various fuels is especially important considering the plurality of SAF pathways currently under investigation.^{14–18}

Three types of elastomer o-rings are designated for testing with novel aviation fuels in ASTM D4054: fluorocarbon (FKM), fluorosilicone (FVMQ), and acrylonitrile-butadiene (NBR, or nitrile rubber).¹⁹ Nitrile rubber has proved to be the most sensitive, and problematic, of these materials regarding o-ring swelling due to variations in fuel composition,^{9,10,20,21} making it a useful subject for research from the perspective of SAF developers. For this reason, in addition to the large regulatory and logistical hurdles associated with material changes on certified, in-service aircraft, the present study investigates property and blending relationships via swell measurements for NBR o-rings only.

ASTM D471²² identifies three methods for quantifying o-ring swell: percent change in mass,^{12,23,24} percent change in dimension,^{24–26} and percent change in tensile strength.^{10,21} This study employs an optical dilatometry technique adapted from Graham²⁴ to measure the change in o-ring sample diameter because of its simplicity, cost-effectiveness, and the small amount of solvent required for testing compared to other methods. Modest heating is shown here to accelerate tests without compromising the results, which is desirable due to the time-consuming nature of o-ring swelling tests relative to other fuel property measurements. While it does not meet the exact specifications for fuel soak tests outlined in Section A3.2.7.2 of ASTM D4054, the efficiency of this method is useful for collecting data for research purposes or low-volume Tier β prescreening testing.²⁷

Currently, the distinction between hydrocarbon classes remains the most telling molecular feature for o-ring swell, with aromatics clearly outperforming *n*-/*iso*-alkanes and cycloalkanes.^{9,10} Of interest to SAF developers due to their low-sooting characteristics, cycloalkanes, specifically polycycloalkanes, have shown promise at high concentrations as potential swell-inducing substitutes for aromatics.^{15,21} Previous work has found qualitative relationships between o-ring swell and decreasing fuel molar volume and molar mass.^{24,26,28} Additionally, steric hindrance (e.g., number or length of alkyl chains) was shown by Romanczyk et al.²⁶ to decrease swelling propensity. Lower o-ring swell from alkanes has been linked to a relative lack of hydrogen bonding and polar forces compared to aromatic compounds, as quantified by Hansen solubility parameters.²⁴ Generally, however, these relationships have not been shown to fully explain the disparity in swelling between hydrocarbon groups. While these relationships offer some direction to SAF developers for molecule selection, more comprehensive testing and model predictions are needed to develop 100%v drop-in SAFs. Made possible by accelerated testing methods, the results reported on the molecules studied here are substantially more diverse than previous studies to enable forecasting of property and compositional relationships.

To date, no extensive evaluation of the linear blending of hydrocarbon mixtures on NBR has been reported in the literature. Here, the accuracy of the linear volumetric blending rule proposed by Kosir et al.²⁰ is assessed to determine its

suitability in modeling applications. Preliminary attempts to quantify blending effects on NBR o-ring swell for molecules doped up to 15%v in an approved alcohol-to-jet (ATJ) SPK SAF product appear to follow the proposed rule.²⁵ This article contains swell measurements at higher dopant concentrations and across several hydrocarbon classes to evaluate linear blending more comprehensively.

This work advances the community knowledge of swelling behavior with 39 molecules blended in an ATJ SPK, documents the repeatability of optical dilatometry experimentation, establishes the linearity of swelling with volumetric composition, and presents some initial first-order modeling of swelling behavior for the 39 compounds. Combined, we present an additional framework for fuel developers to understand the compositional effects of fuel on elastomeric material compatibility in an effort to produce 100%v “drop-in” SAF.

2. MATERIALS AND METHODOLOGY

2.1. Materials. Hand-cut, thin cross-sectional slices of size 216 Parker-Hannifin nitrile rubber o-rings procured from Zatkoff Seals & Packaging were used as elastomer samples for swell measurements. Because the focus of this study is to inform SAF developers about swell-inducing fuel components, nitrile rubber’s sensitivity to fuel composition is leveraged to emphasize swell–property relationships and blending effects. This study uses nitrile rubber o-ring swell measurements with 56 total solvents, including 39 neat molecules doped at 8%v in an approved SAF, 14 conventional fuels, 3 SAF blend components, and 2 blends of conventional fuel with SAF.

Thirty-nine chemicals, listed in Table 1, were employed for o-ring swell measurement in this work. Of these molecules, there are 20 aromatics (14 alkylbenzenes, 2 cycloaromatics, 3 naphthalenes, and biphenyl), and 19 cycloalkanes (16 monocycloalkanes and 3 polycycloalkanes). Informed by the molar volume correlation found in the literature, a focus was put on selecting molecules representing the jet fuel volatility range for each hydrocarbon class. *N*-/*iso*-alkanes were not evaluated as dopant molecules here because they are known to have an insignificant influence on o-ring swell.^{9,10,29,30}

Eleven different shipments of petroleum-based jet fuel used in an extensive report on this topic⁹ along with three additional samples of petroleum fuels from the National Jet Fuels Combustion Program (NJFCP)³¹ were used to set a three-standard deviation experience range for the o-ring swelling activity of conventional jet fuel. The aromatics fraction of these fuels varies between 11.9 and 23.1%v. For comparison, the population distribution of aromatics concentration in 1434 samples of JP-8 analyzed in 2011 showed a range of 7.0–24.5% v.³² The compositional variance between manufacturing batches of nitrile rubber o-rings is also significant,³³ rendering it necessary to reestablish the conventional swell range for each batch received. For this reason, all of the measurements presented in this work were performed on o-ring samples cut from the same manufacturing batch of o-rings.

The three-standard deviation range for these conventional jet fuels with the batch of o-rings used in this study is 8.3–17.1%v/v. Because of the difference in aromatics concentration between our experiment population, the 2011 field population distribution, and the limited operational experience of observed fuel leakage^{1,12} it is unclear whether this captures the full range of conventional jet fuel swelling activity. Nonetheless, this range offers a useful reference for prescreening and research-related swell measurements.

Two SAF products listed in ASTM D7566 and approved up to 50% v with previously qualified Jet-A were used in this study: Gevo ATJ (SPK from *iso*-butanol and also labeled as C-1) and World Energy HEFA (SPK from hydroprocessed esters and fatty acids). These fuels are predominantly made up of *n*- and *iso*-alkanes and thus exhibit very low swelling. Their swell characteristics make these SAFs useful for showcasing potential dopant molecules and blends that can improve low-swelling fuels in relation to the conventional swell range. Lastly,

Table 2. 3 Conventional Fuels and 3 SAF Blend Components Used in This Study with Tabulated Aromatic Content, Molar Volume, Density, and Converged Seal Swell

fuel name	POSF	producer	aromatic content [%v]	molar volume [mL/mol]	density at 15 °C [kg/m ³]
A-1	10264	NuStar Refining	11.9	194.9	779.9
A-2	10325	Shell Mobile	16.4	198.9	803.5
A-3	10,289	Valero	18.4	200.8	826.8
C-1	13718	Gevo	<1	237.4	758.2
HEFA	n/a	World Energy (WE)	<1	214.3	751.4
SAK/HEFA 21/79	n/a	Virent/WE	20.1	150.4	776.1

the 21/79%v SAK/HEFA blend studied by Feldhausen et al.¹⁴ was included in this study as an example of a 100%v SAF blend from two pathways that meet ASTM D7566 specifications and conventional swell levels. Relevant details regarding these fuels are listed in Table 2.

In an effort to save space, information for the eleven additional shipments of approved petroleum-based jet fuel used to establish the conventional swell range for this study are tabulated with their converged swell measurements in the Supporting Information.

2.2. Seal Swell Measurement. Optical dilatometry, first applied to seal swell measurements by Graham²⁴ and utilized further by Kosir et al.²⁰ is employed here to measure the change in the cross-sectional area of o-ring slices that are submerged in a vial filled with 5 mL of solvent. The vial is capped to prevent evaporation and is placed on a custom-built dilatometer. The initial area of the o-ring sample is extrapolated from 13 pictures taken 20 s apart using the time expired between o-ring contact with the solvent and the first picture taken. After the first 4 min, pictures are taken every 10 min until convergence is observed with respect to the o-ring swell. Image processing software is used to record the area of the o-ring sample in pixels. The volume is determined by eq 1 from Graham et al.²⁸ where V_i is o-ring swell, in %v/v, of a given image, A_i is the o-ring area for a given image, and A_0 is the o-ring area when it is first submerged in the vial. The reported converged seal swell is the average of the last 30 pictures collected. It is assumed that the o-ring slices swell isotropically.

$$V_i = 100 \left[\left(\frac{A_i}{A_0} \right)^{3/2} - 1 \right] \quad (1)$$

Tests are run at room temperature (22 ± 1.0 °C) or in a custom-built oven heated to maintain an internal temperature of 37.15 ± 0.45 °C, just below the minimum flash point of jet fuel.⁵ Heated tests are designed to reach convergence with reduced testing time, as the test duration is a major factor contributing to the rate of progress in this area of research. The oven consists of a two-part insulated enclosure, with each compartment containing 5 optical dilatometry test stands and a 120 V/120 W silicone heater manufactured by Tutco-Farnam. Any temperature cycling has been found to occur within the listed values over the course of 24 h, which is likely a result of minor building temperature changes between working and nonworking hours.

Swell tests are considered converged when the swell remains nominally unchanged over at least 24 h, which typically occurs after 10–14 days at room temperature, or 5–10 days at 37 °C. Minor differences were noted between the converged swell of heated and nonheated tests for A-2, A-1, HEFA, and C-1, but efforts to determine a consistent trend in results were inconclusive. For this reason, the present study uses a flat repeatability uncertainty of $\pm 0.59\%$ v/v derived from the combined results of 6 heated and 11 room temperature tests of A-2 to account for any experimental variation, including temperature and o-ring sample size. Data for these repeatability efforts, the heater temperature cycle, and the overall experimental setup and workflow can be found in the Supporting Information.

3. RESULTS

Figure 1 shows the behavior of the nitrile rubber o-ring swell tests over the first two weeks of measurement for the molecules reported in Table 1 doped at 8%v in C-1. Each test is designated by either the solvent's molar volume (Figure 1a,b) or density (Figure 1c,d) using a normalized color bar for each property. Additionally, the average conventional fuel swell (solid-black line) and 3σ conventional range (blue-shaded region), and the neat C-1 swell (dashed-black line) are shown for reference. All measurements discussed in this section, except for the solvents doped with cycloaromatics, naphthalenes, and biphenyl, have bulk density values calculated via the blending rule to be below the ASTM minimum density requirement (775 kg/m^3)⁵ because C-1 (758.2 kg/m^3) is used at 92%v in each, which is a substantially higher volume fraction than what would be present in jet fuel under the current 50%v SAF blending limit.

The purpose of the color bar here is to visualize the adherence of the raw data in this study to the molar volume correlation in the literature and the density. A strong correlation to these trends would take the form of a natural gradient of purple-blue to green-yellow from top to bottom, whereas a weak correlation would result in near-random ordering of these colors. The reversal of the color bar to the right of the plots is to maintain the same color gradient in the data for each property while accommodating for decreasing and increasing swell relationships with molar volume and density, respectively.

As observed by Graham,²⁴ o-ring swelling as a function of time is a result of two processes: fuel absorption by the elastomer and material extraction by the fuel. This is apparent in Figure 1 where each test undergoes a period of rapid swelling within the first hours of contact with a fuel blend before gradually shrinking over the remainder of the test period as the fuel behaves as a solvent for the plasticizer material found in elastomer o-rings. The number of species investigated here for converged swell provides useful foundations for future study of these processes, which are important due to the impacts of fuel cycling on o-ring swelling.

Figure 2 presents the converged NBR swell measurements for the molecules listed in Table 1 doped at 8%v in C-1 and grouped by hydrocarbon class. The 8%v dopant concentration was chosen to assess both the swelling effect of the individual molecules and the 8%v minimum aromatics requirement as a surrogate requirement to long-duration, measured o-ring swell. The green shaded region represents the 3-sigma conventional fuel swell range found with the batch of NBR o-rings used for this study (8.3–17.1%v/v). The results displayed in Figure 2 can also be found in tabulated format in the Supporting Information.

The accuracy of a linear volumetric blending rule for o-ring swell was studied using 4 molecules, *n*-butylcyclohexane, *n*-

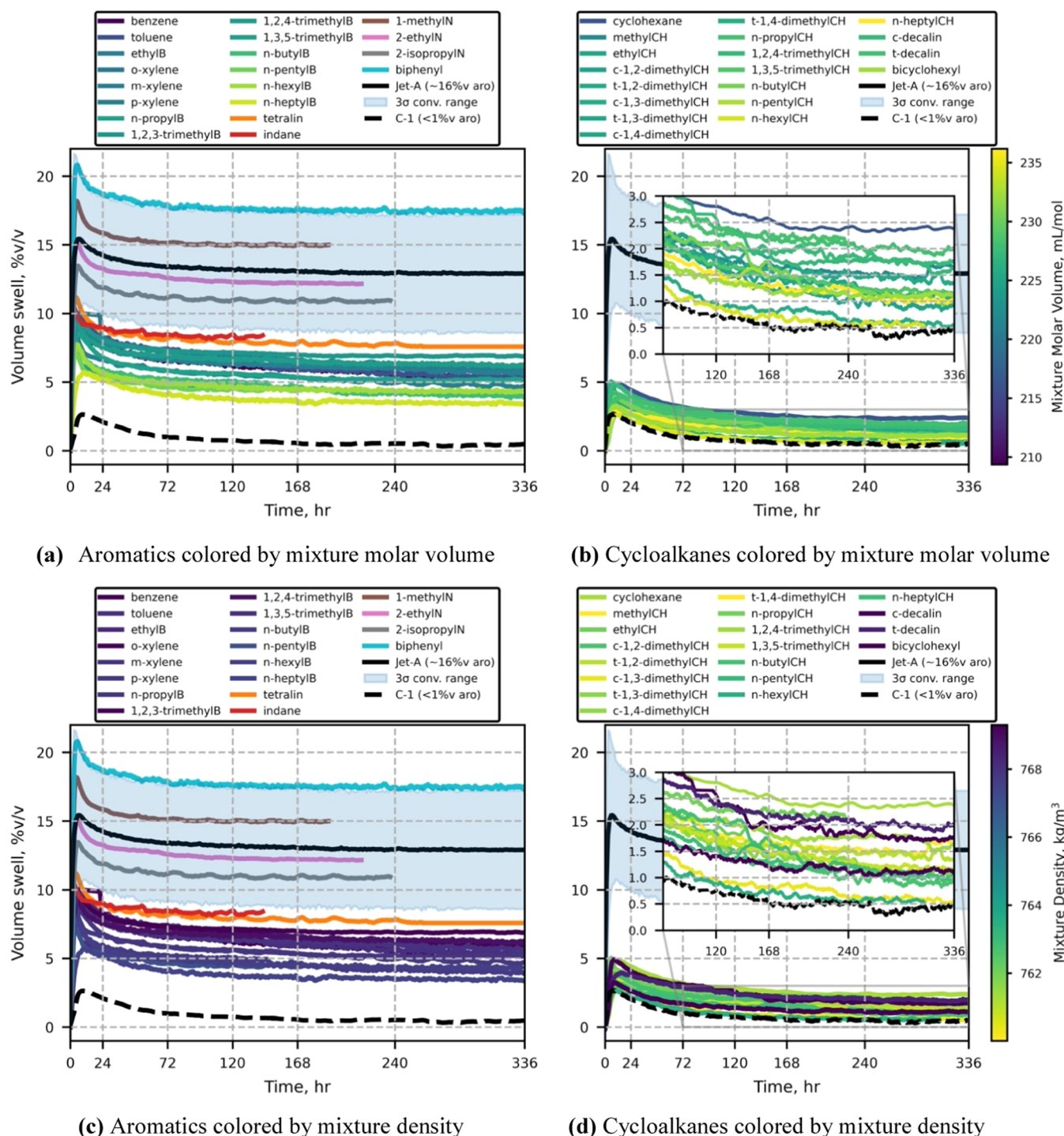


Figure 1. O-ring seal swell over time for aromatics (a, c) and cycloalkanes (b, d) doped at 8%v in C-1. In plots (a, c), cyclo-aromatic, naphthalene, and biphenyl-doped mixtures are identified by colors outside of the color gradient because their relatively extreme property values change the scaling of the color bar such that the alkylbenzenes and cycloalkanes become indistinguishable from each other. Cycloalkane plots (b, d) include zoomed inset plots to provide clarity for overlapping data.

propylbenzene, tetralin, and 2-ethylnaphthalene doped at 3, 5, 8, 10, 15, 25, and 40%v in C-1. These molecules were selected to represent the majority of the hydrocarbon classes in Table 1. Table 3 lists the converged swell measurements for the blending rule portion of this study.

4. ANALYSIS AND DISCUSSION

4.1. Impact of Hydrocarbon Class on O-Ring Swell.

The results in Figure 2 show consistency with the literature for the swelling propensity of each hydrocarbon class. Dopants consisting of multiple aromatic rings (biphenyl and naphthalenes) had the highest swelling effect. These are followed, in order, by the cyclo-aromatic, alkylbenzene, polycycloalkane, and monocycloalkane dopants. The range of swell appears

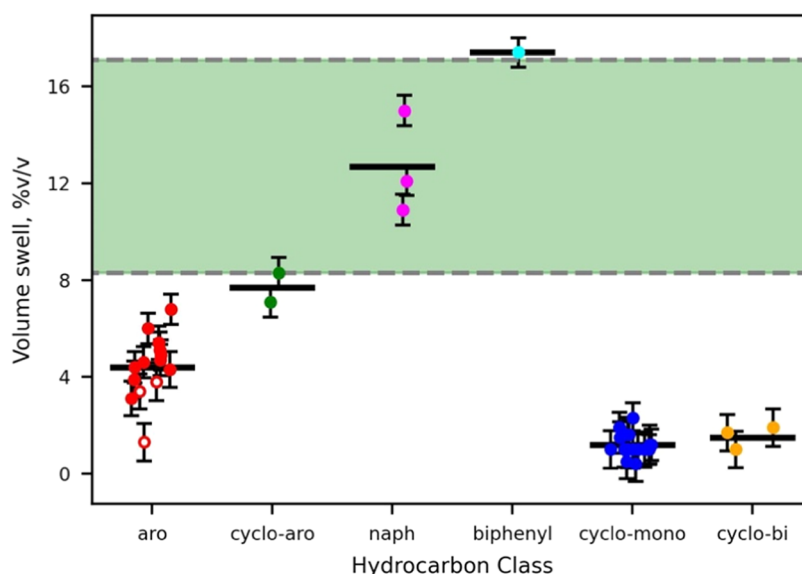


Figure 2. Converged swell measurements for molecules listed in Table 1 doped at 8%v in Gevo C-1 and grouped by hydrocarbon class. Black bars represent the average swell for each hydrocarbon class. Open circles represent final swell measurements for unconverged runs that were terminated due to time considerations.

Table 3. Converged Swell Results (%v/v) at Every Concentration in the Blending Rule Test Series

dopant	3%v	5%v	8%v	10%v	15%v	25%v	40%v
<i>n</i> -butylcyclohexane	1.4	1.6	1	2.1	2.3	3.3	4.2
<i>n</i> -propylbenzene	2.5	4.3	4.9	6.5	8.9	13.3	20.7
tetralin	3.4	4.1	7.1	8.3	14.8	21.7	38.8
2-ethylnaphthalene	4.9	7.5	12.1	16.8	25.0	40.3	65.4

distinct between each hydrocarbon class, other than the similarity in swelling between mono- and polycycloalkanes, highlighting that properties that differentiate these classes are good starting points for the search of properties with an effect on o-ring swell. The average swell and standard deviation for each hydrocarbon class in Figure 2 (excluding biphenyl) can be found in Table 4.

Table 4. Average Swell and Standard Deviation for Molecules in Table 1 Doped at 8%v in C-1 Grouped by Hydrocarbon Class

hydrocarbon class	average swell [%v/v]	standard deviation [%v/v]
alkylbenzenes ^a	4.8	1.00
cycloaromatics	7.7	0.85
naphthalenes	12.7	2.11
monocycloalkanes	1.2	0.48
polycycloalkanes	1.5	0.47

^aThe calculation of average swell for alkylbenzenes omits the mixtures doped with benzene, toluene, and *m*-xylene because they did not converge.

It is important to point out that any work providing guidance to fuel developers to meet operability standards should consist of measurements on industry-relevant compounds and fuels. The dopants studied here have either been identified in current SAF,¹⁴ reported as relevant SAF compounds for producers,³⁴ or are structurally similar to compounds in either of these categories. These compounds, as well as the neat fuels measured, were strategically chosen to show fuel producers multiple pathways to elastomer

compatibility using a range of producible fuel blend components rather than recommending a small number of specific dopants.

The converged swell measurements also show that the 8%v alkylbenzene-doped mixtures and a 50/50%v C-1/A-2 blend (found in Figure 3) do not meet the conventional swell range found in this work. Two possible explanations for this related to the composition of the conventional fuel samples used here have been identified. The first is the relatively high aromatics concentration in these fuels compared to that of the larger population described in Section 2.1. The second is the uncharacterized concentration of heteroatom-containing compounds in these conventional fuel samples. Trace amounts of heteroatom-containing compounds, especially those containing nitrogen and oxygen, significantly increase o-ring swell^{26,28,35,36} and as a result could drive the conventional swell range found here higher. These factors give insight into the number of factors influencing o-ring swell and highlight a potential benefit of using o-ring swell measurements as a quality control metric in lieu of the 8%v aromatics limit.

The variation in swelling of the alkylbenzene-doped mixtures implies that property relationships can be leveraged to select aromatics that will increase SAF o-ring swell relative to the typical distribution of aromatic species in conventional jet fuel when doped at the same concentration. Due to the larger effect of experimental repeatability on the measurement precision for lower swelling molecules, it is not currently possible to make similar conclusions for the variation in cycloalkane swelling. Overcoming this obstacle is especially of interest for characterizing polycycloalkanes, specifically decalins, due to their potential to increase the swelling propensity and density of

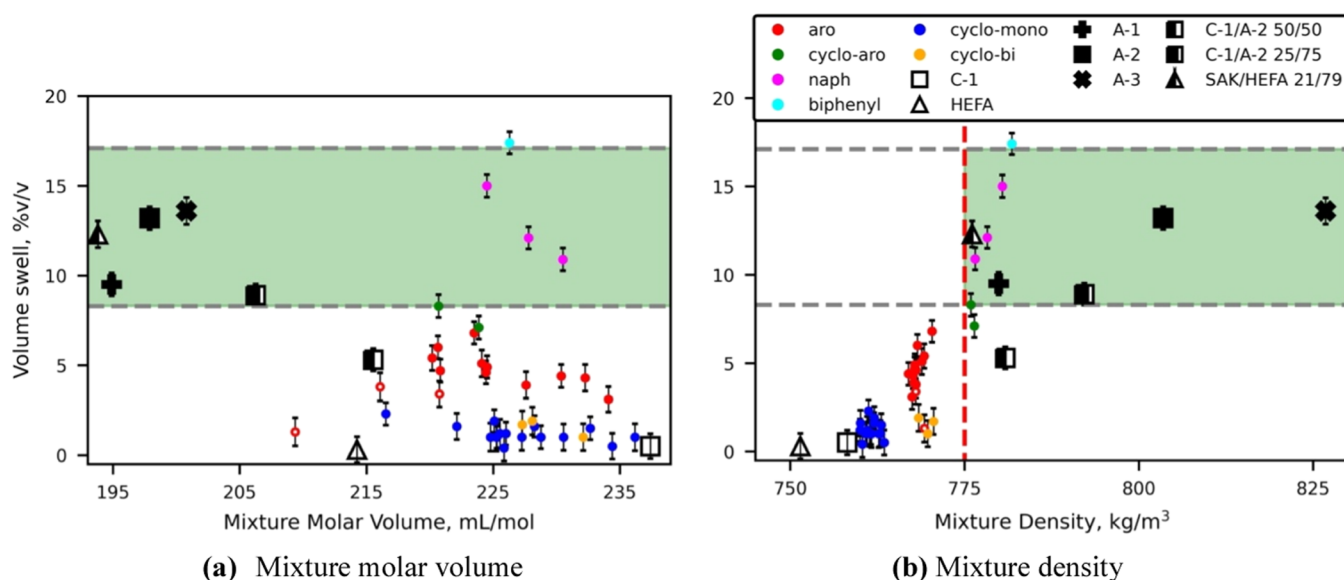


Figure 3. Scatter plots depicting the final seal swell for each molecule doped at 8%v in C-1 compared to the molar volume (a) or density (b) of the mixture calculated via blending rule. Empty circular markers represent the tests in this study whose swell did not converge. Gray dashed lines represent the limits of the conventional swell range, and the red dashed line in (b) is indicative of the ASTM D7566 minimum density specification.

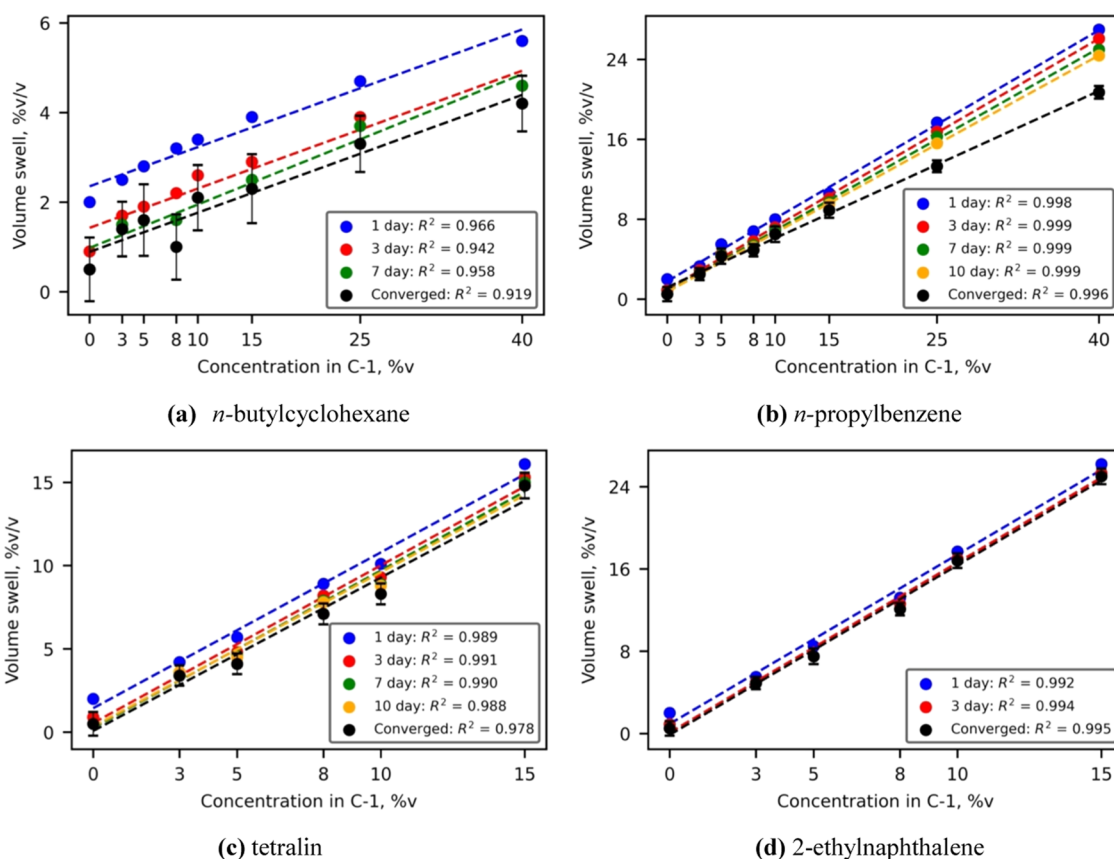


Figure 4. (a–d) Scatter plots presenting the seal swell of 4 different dopants (listed beneath each subplot) in C-1 at concentrations ranging from 3 to 40%v, along with a neat C-1 measurement. Each color marker and trendline represents the swell at a different timestep during the test. Note the different swell ranges on each subplot.

SAF without negatively impacting sooting.³⁷ More precise characterization of the swelling effect from aliphatic compounds may be possible via other methods of swell measurement such as compositional data,^{24,35} tensile

strength,^{10,21,26} or a combination of these with optical dilatometry.

4.2. Swell Relationships with Molar Volume and Density. Figure 3 features scatter plots of the converged swell results of the mixtures in Figure 2, the fuels in Table 2, and C-

Table 5. Average (Average Hydrocarbon Class Swell as Reported in Table 4), Minimum (Highest Swell), and Maximum (Lowest Swell) Volume Fraction of a Single Dopant in a Binary Mixture with C-1 Projected to Meet the Minimum Conventional Swell Found Here (8.3%v/v)^a

dopant hydrocarbon class	average concentration [%v]	minimum concentration [%v]	maximum concentration [%v]	average TSI ³⁷
alkylbenzenes	13.8	9.8	21.4 ^b	55.4
cycloaromatics	8.6	8.0	9.4	61.6
naphthalenes	5.2	4.4	6.1	100.1
monocycloalkanes	55.3	28.9	n/a ^c	7.7
polycycloalkanes	44.3	34.9	66.4	16.7

^aAverage neat dopant TSI is also included to give reference on the emissions impact of the blend component. ^bThe measurement for *n*-heptylbenzene was used for this scenario because it is the lowest swell measurement for alkylbenzene dopants that fully converged. ^cThe lowest swelling monocycloalkane dopants are not projected by this analysis to meet the minimum conventional o-ring swell level at any concentration in C-1.

1/A-2 blends at 25/75 and 50/50%v ratios as they relate to molar volume (Figure 3a) and density (Figure 3b). This data is consistent with the literature in that higher swell is observed with decreasing molar volume within hydrocarbon classes, but for modeling purposes, it is useful to identify more general property relationships. These visualizations indicate that o-ring swell is significantly more linear with density for all hydrocarbon classes, barring polycycloalkanes, than it is with molar volume. This may be the result of density confounding two properties, molar mass and molar volume, known to impact swelling. Factoring in both of these properties has an advantage over molar volume alone because it accounts for the degree of saturation of the carbon atoms, a major differentiator between hydrocarbon classes, and the structural connectivity of the molecule.

The alkylbenzene-doped mixtures exhibit lower density than the minimum requirement for jet fuel denoted by the red dashed line in Figure 3b. While this is the result of the volume fraction of C-1 exceeding the SAF blending limit, higher-density SPK SAF products could provide the opportunity to reach the minimum density requirement when doped with aromatics at similar ratios. This calls attention to the fact that each pathway, and even different fuels within a single pathway, can have property differences and benefit from direct quantification to evaluate suitability for increased blending with conventional fuel.

Swell relationships universal across hydrocarbon classes, such as the density correlation identified here, directly benefit the prediction and understanding of o-ring swell for jet fuel based on compositional data. Future modeling efforts will benefit from investigating other swell–property relationships of this type, including explaining the low swell from polycycloalkanes given their high density. Any such modeling requires the quantification of seal swell as it relates to the concentration of a dopant molecule from a given hydrocarbon class.

4.3. Linear Volumetric Blending Rule. Figure 4 shows converged o-ring swell plotted for each dopant/C-1 mixture listed in Table 3, in addition to the swell at 1-, 3-, 7-, and 10-day timesteps when available. The results for each timestep are characterized by a linear trendline with a reported coefficient of determination (R^2) to evaluate changes over the duration of the swelling process. The results for tetralin and 2-ethyl-naphthalene at 25 and 40%v are excluded because their extremely high swell is far off the scale used here to highlight differences between data taken at different time intervals. Trendline slope information from Figure 4 is tabulated in the Supporting Information.

All linear trendlines resulted in an R^2 of 0.919 or higher, corroborating the linear blending rule proposed by Kosir et al.²⁰ for predicting o-ring swell. The representative cycloalkane for this study, *n*-butylcyclohexane, produced a noticeably lower R^2 value compared to the aromatics studied. A possible reason for this is the larger relative uncertainty inherent in the swell tests of molecules exhibiting lower swell, which will require a more thorough assessment for a large number of species and concentrations outside the scope of this study. In light of this, a linear relationship with concentration is still recommended to avoid overfitting, while capturing the main effects of blending on o-ring swell.

The timesteps in Figure 4 illustrate an opportunity to further decrease the time required to collect valuable information from swell experiments. Because the linearity of these timesteps does not significantly vary in slope and R^2 value for a single dopant, it may be possible to predict converged o-ring swell at any blend ratio based on a converged data point at one concentration, and a concentration series of data points evaluated one day into the experiment.

Linear blending is employed to estimate the volume fraction of dopant needed to achieve 8.3%v o-ring swell, which is the bottom of the 3-sigma range determined in this work. Results are presented in Table 5 for the average, highest, and lowest swelling representative of each of five classes evaluated here as potential dopants. Among these classes, alkylbenzenes and cycloalkanes have less deleterious impacts with regard to sooting propensity compared to naphthalenes (limited to 3%v in jet fuel for this reason⁵) or cycloaromatics. This property is quantified here using methods established by Boehm et al.³⁷ to predict the average threshold sooting index (TSI) prediction for the pure dopant molecule in each hydrocarbon class.

As expected, significantly larger fractions of cycloalkanes are required to achieve adequate swell than that of alkylbenzenes. Because post-production blending to increase the swell of SAF such as C-1 or HEFA poses added costs, it is desirable to minimize the fraction of blend component required without significantly increasing the TSI of the fuel. The scenarios presented in Table 5 exhibit sizeable differences in dopant concentration based on molecule selection, highlighting the importance of using property relationships to identify the most efficient swell blend components and potential low- or zero-aromatic fuel compositions. Additional investigation into blending for more molecules, ratios, and complex mixtures will help develop these tools into a more comprehensive model for swell prediction.

5. CONCLUSIONS

Due to the difficulty associated with large-scale material changes in aircraft, the advancement of “drop-in” SAF is heavily reliant on the compatibility of fuels with nitrile rubber o-ring swelling. The present work addresses this through the investigation of fuel compositional and property relationships with optical dilatometry measurements of nitrile rubber o-ring swell for 56 total solvents, including 39 neat molecules doped in an approved SPK SAF, 14 conventional fuels, 3 SAF blend components, and 2 blends of conventional fuel with SAF to investigate compositional and molecular property relationships with swelling. Swell measurements for neat molecules doped at 8%v in an approved SPK SAF, Gevo C-1, exhibited consistency with literature trends with molar volume and dopant hydrocarbon class. These tests also revealed a relationship between o-ring swell and density that showed more linearity than the previous correlation with molar volume across hydrocarbon classes, except for polycycloalkanes, which illustrate a need for more swell–property relationship investigations of this type. Similar linearity was also observed with density for blends of conventional fuels and SAFs.

Coupled with these property relationships was the verification that linear volumetric blending is applicable for o-ring swelling for active components up to 40%v in C-1. Linear blending was then applied to demonstrate changes in fuel composition required for sufficient o-ring swell due to variance in swelling propensity within hydrocarbon classes, highlighting the importance of using property relationships and swell measurements to inform efficient blend component selection without negative impacts on the TSI of the fuel.

The data reported here guides SAF developers toward 100% v “drop-in” SAF by predicting material compatibility of proposed SAF dopants and compositions based on molecular properties and concentration.

■ ASSOCIATED CONTENT

SI Supporting Information

The Supporting Information is available free of charge at <https://pubs.acs.org/doi/10.1021/acs.energyfuels.3c00781>.

Converged swell results for the neat fuels, conventional/SAF blends, neat and molecules doped at 8%v in Gevo C-1 used in this work (Table S1); aromatic content and converged results for 11 conventional fuel samples provided by Dr. Graham of UDRI that were used in addition to the 3 “A” fuels in Table S1 to determine the 3-sigma conventional fuel range for this study (Table S2); trendline slope information for the linear blending study (Table S3); plots demonstrating the repeatability of heated and nonheated optical dilatometry methods (Figures S1 and S2); plot demonstrating repeatability over an intentionally wide range of o-ring sample masses (Figure S3); heated test temperature cycle data (Figure S4); and diagram of optical dilatometry and experimental setup (Figure S5) (PDF)

■ AUTHOR INFORMATION

Corresponding Authors

Conor Faulhaber – *Bioproducts, Sciences, and Engineering Laboratory, School of Engineering and Applied Science, Washington State University, Richland, Washington 99354, United States; Mechanical and Aerospace Engineering, University of Dayton, Dayton, Ohio 56469-0238, United*

States; orcid.org/0009-0003-5634-0864;

Email: conor.faulhaber@wsu.edu

Joshua Heyne – *Bioproducts, Sciences, and Engineering Laboratory, School of Engineering and Applied Science, Washington State University, Richland, Washington 99354, United States; Energy Processes and Materials Division, Energy and Environment Directorate, Pacific Northwest National Laboratory, Richland, Washington 99352, United States*; orcid.org/0000-0002-1782-9056;
Email: joshua.heyne@wsu.edu

Authors

Christopher Borland – *Mechanical and Aerospace Engineering, University of Dayton, Dayton, Ohio 56469-0238, United States*

Randall Boehm – *Bioproducts, Sciences, and Engineering Laboratory, School of Engineering and Applied Science, Washington State University, Richland, Washington 99354, United States*; orcid.org/0000-0003-2983-1337

Complete contact information is available at:

<https://pubs.acs.org/10.1021/acs.energyfuels.3c00781>

Author Contributions

C.F.: conceptualization, data curation, formal analysis, investigation, methodology, resources, validation, visualization, writing—original draft, writing—review and editing. C.B.: conceptualization, investigation, methodology, software, validation, writing—review and editing. R.B.: formal analysis, supervision, writing—review and editing. J.H.: conceptualization, funding acquisition, project administration, writing—review and editing.

Notes

The authors declare no competing financial interest.

■ ACKNOWLEDGMENTS

The authors acknowledge funding from the U.S. Federal Aviation Administration Office of Environment and Energy through ASCENT, the FAA Center of Excellence for Alternative Jet Fuels and the Environment, project 65 through FAA Awards 13-CAJFE-UD-026 and 13-CAJFE-WASU-035 (PI: Dr. Joshua Heyne) under the supervision of Dr. Anna Oldani. Any opinions, findings, conclusions, or recommendations expressed in this material are those of the authors and do not necessarily reflect the views of the FAA or other sponsors. The authors also thank Dr. John Graham of UDRI for providing reference conventional jet fuel samples, Shane Kosir for assistance with methods development, and Zhibin Yang for contributing toward data collection.

■ NOMENCLATURE

A_0 = initial o-ring area, in pixels, extrapolated from first ten measured areas

A_i = measured o-ring area, in pixels, at time i

ASTM = ASTM International

ATJ = alcohol-to-jet fuel pathway

FID = flame ionization detector

GCxGC = two-dimensional gas chromatography

HEFA = hydroprocessed esters and fatty acids

NJFCP = National Jet Fuel Combustion Program

R^2 = coefficient of determination

SAF = sustainable aviation fuel

SAK = synthetic aromatic kerosene

SPK = synthetic paraffinic kerosene
TSI = threshold sooting index
 V_i = calculated o-ring volume swell at time i
VUV = vacuum ultraviolet light detector
%v = volume percentage
%v/v = o-ring volume swell percentage relative to the initial volume

REFERENCES

- (1) "Report on the Feasibility of a Long-Term Aspirational Goal (LTAG) for International Civil Aviation CO₂ Emission Reductions," International Civil Aviation Organization. Mar. 2022. Accessed: Jan. 25, 2023. [Online]. Available: https://www.icao.int/environmental-protection/LTAG/Documents/REPORT%20ON%20THE%20FEASIBILITY%20OF%20A%20LONG-TERM%20ASPIRATIONAL%20GOAL_en.pdf.
- (2) "A4A Climate Change Commitment and Flight Path: Innovative Industry and Government Action to Achieve Net-Zero Carbon Emissions," Airlines for America. Mar. 2021. Accessed: Dec. Jan. 25, 2023 [Online]. Available: <https://www.airlines.org/wp-content/uploads/2021/05/A4A-Climate-Change-Commitment-Flight-Path-to-Net-Zero-FINAL-3-30-21.pdf>.
- (3) SAF Grand Challenge Roadmap Flight Plan for Sustainable Aviation Fuel, 2022. <https://www.energy.gov/sites/default/files/2022-09/beto-saf-gc-roadmap-report-sept-2022.pdf>. Accessed: January 25, 2023.
- (4) Balancing growth in connectivity with a comprehensive global air transport response to the climate emergency: a vision of net-zero aviation by mid-century, 2020. https://aviationbenefits.org/media/167187/w2050_full.pdf. Accessed: December. 10, 2022.
- (5) Designation: D7566 – 22a Standard Specification for Aviation Turbine Fuel Containing Synthesized Hydrocarbons 1; American Society for Testing and Materials, 2022.
- (6) Kramer, S.; Andac, G.; Heyne, J.; Ellsworth, J.; Herzig, P.; Lewis, K. C. Perspectives on Fully Synthesized Sustainable Aviation Fuels: Direction and Opportunities. *Front. Energy Res.* **2022**, *9*, No. 1040.
- (7) Lee, D. S.; Fahey, D. W.; Skowron, A.; Allen, M. R.; Burkhardt, U.; Chen, Q.; Doherty, S. J.; Freeman, S.; Forster, P. M.; Fuglestedt, J.; et al. The contribution of global aviation to anthropogenic climate forcing for 2000 to 2018. *Atmos. Environ.* **2021**, *244*, No. 117834.
- (8) Voigt, C.; Kleine, J.; Sauder, D.; Moore, R. H.; Bräuer, T.; Le Clercq, P.; Kaufmann, S.; Scheibe, M.; Jurkat-Witschas, T.; Aigner, M.; et al. Cleaner burning aviation fuels can reduce contrail cloudiness. *Commun. Earth Environ.* **2021**, *2*, No. 114.
- (9) Graham, J. L.; Rahmes, T. F.; Kay, M. C.; Belières, J. P.; Kinder, J. D.; Millett, S. A.; Vannice, W. L.; Trela, J. A. *Impact of Alternative Jet Fuel and Fuel Blends on Non-Metallic Materials Used in Commercial Aircraft Fuel Systems Continuous Lower Energy, Emissions and Noise (CLEEN) Program*; Boeing Company, 2011.
- (10) Anuar, A.; Undavalli, V. K.; Khandelwal, B.; Blakey, S. Effect of fuels, aromatics and preparation methods on seal swell. *Aeronaut. J.* **2021**, *125*, 1542–1565.
- (11) Anderson, B. E.; Beyersdorf, A. J.; Hudgins, C. H.; Plant, J. V.; Thornhill, K. L.; Winstead, E. L.; Ziemba, L. D.; Howard, R.; Corporan, E.; Miake-Lye, R. C. et al. Alternative Aviation Fuel Experiment (AAFEX), NASA Glenn Research Center. Cleveland, Ohio, 2011. <https://ntrs.nasa.gov/api/citations/20110007202/downloads/20110007202.pdf>.
- (12) Forzono, C. Fuel System O-Ring Leaks on Post P.D.M. (Programmed Depot Maintenance) C-5A Aircraft, Kelly Air Force Base, Texas, 1983. https://ia800108.us.archive.org/9/items/DTIC_ADA137885/DTIC_ADA137885.pdf.
- (13) Yamabe, J.; Fujiwara, H.; Nishimura, S. Fracture Analysis of Rubber Sealing Material for High Pressure Hydrogen Vessel. *J. Environ. Eng.* **2011**, *6*, 53–68.
- (14) Feldhausen, J.; Bell, D. C.; Yang, Z.; Faulhaber, C.; Boehm, R.; Heyne, J. Synthetic aromatic kerosene property prediction improvements with isomer specific characterization via GCxGC and vacuum ultraviolet spectroscopy. *Fuel* **2022**, *326*, No. 125002.
- (15) Yang, Z.; Xu, Z.; Feng, M.; Cort, J. R.; Gieleciak, R.; Heyne, J.; Yang, B. Lignin-based jet fuel and its blending effect with conventional jet fuel. *Fuel* **2022**, *321*, No. 124040.
- (16) Huq, N. A.; Hafenstine, G. R.; Huo, X.; Nguyen, H.; Tiffit, S. M.; Conklin, D. D.; Stück, D.; Stunkel, J.; Yang, Z.; Heyne, J.; et al. Toward net-zero sustainable aviation fuel with wet waste-derived volatile fatty acids. *Proc. Natl. Acad. Sci. U.S.A.* **2021**, *118*, No. e2023008118.
- (17) Cronin, D. J.; Subramaniam, S.; Brady, B.; Cooper, A.; Yang, Z.; Heyne, J.; Drennan, C.; Ramasamy, K. K.; Thorson, M. R. Sustainable Aviation Fuel from Hydrothermal Liquefaction of Wet Wastes. *Energies* **2022**, *15*, No. 1306.
- (18) Stone, M. L.; Webber, M. S.; Mounfield III, W. P.; Bell, D. C.; Christensen, E.; Morais, A. R. C.; Li, Y.; Anderson, E. M.; Heyne, J.; Beckham, G. T.; Román-Leshkov, Y. Continuous hydrodeoxygenation of lignin to jet-range aromatic hydrocarbons. *Joule* **2022**, *6*, 2324–2337.
- (19) Designation: D4054 – 22 Standard Practice for Evaluation of New Aviation Turbine Fuels and Fuel Additives 1; American Society for Testing and Materials, 2022.
- (20) Kosir, S. T.; Heyne, J.; Graham, J. L. A machine learning framework for drop-in volume swell characteristics of sustainable aviation fuel. *Fuel* **2020**, *274*, No. 117832.
- (21) Liu, Y.; Wilson, C. W. Investigation into the impact of n-decane, decalin, and isoparaffinic solvent on elastomeric sealing materials. *Adv. Mech. Eng.* **2012**, *4*, No. 127430.
- (22) Designation: D471 – 16a Standard Test Method for Rubber Property—Effect of Liquids; American Society of Testing and Materials, 2021.
- (23) Muzzell, P.; Stavinoha, L.; Chapin, R. Synthetic Fischer Tropsch (FT) JP-5/JP-8 Aviation Turbine Fuel Elastomer Compatibility Final Report, Defense Technical Information Center, 2004. <https://apps.dtic.mil/sti/citations/ADA477802>.
- (24) Graham, J. L. *The Swelling of Nitrile Rubber by Selected Species in a Synthetic Jet Turbine Fuel*; University of Dayton, 2006.
- (25) Faulhaber, C.; Kosir, S. T.; Borland, C.; Gawełek, K.; Boehm, R.; Heyne, J. In *Optical Dilatometry Measurements for the Quantification of Sustainable Aviation Fuel Materials Compatibility*, AIAA SCITECH 2022 Forum; ARC, 2022.
- (26) Romanczyk, M.; Velasco, J. H. R.; Xu, L.; Vozka, P.; Dissanayake, P.; Wehde, K. E.; Roe, N.; Keating, E.; Kilaz, G.; Trice, R. W.; et al. The capability of organic compounds to swell acrylonitrile butadiene O-rings and their effects on O-ring mechanical properties. *Fuel* **2019**, *238*, 483–492.
- (27) Yang, Z.; Kosir, S.; Stachler, R.; Shafer, L.; Anderson, C.; Heyne, J. A GC × GC Tier α combustor operability prescreening method for sustainable aviation fuel candidates. *Fuel* **2021**, *292*, No. 120345.
- (28) Graham, J. L.; Striebich, R. C.; Myers, K. J.; Minus, D. K.; Harrison, W. E., III Swelling of nitrile rubber by selected aromatics blended in a synthetic jet fuel. *Energy Fuels* **2006**, *20*, 759–765.
- (29) Graham, J. L.; Striebich, R. C.; Minus, D. K.; Harrison III, W. E. In *A Statistical Approach to Estimating the Compatibility of Alternative Fuels with Materials used in Seals and Sealants*, 43rd AIAA/ASME/SAE/ASEE Joint Propulsion Conference & Exhibit, 2007.
- (30) Liu, Y.; Wilson, C. W.; Blakey, S.; Dolmansley, T. Elastomer Compatibility Test of Alternative Fuels Using Stress Relaxation Test and FTIR Spectroscopy, ASME Turbo Expo, Vancouver, British Columbia, 2011. <http://proceedings.asmedigitalcollection.asme.org/pdfaccess.ashx?url=/data/conferences/gt2011/70296/>.
- (31) Colket, M.; Heyne, J.; Rumizen, M.; Gupta, M.; Edwards, T.; Roquemore, W. M.; Andac, G.; Boehm, R.; Lovett, J.; Williams, R.; et al. Overview of the national jet fuels combustion program. *AIAA J.* **2017**, *55*, 1087–1104.

(32) Martin, D.; Wilkins, P. *Petroleum Quality Information System (PQIS) 2011 Annual Report*; DLA Energy: Fort Belvoir, Virginia, 2011.

(33) Parker Hannifin Corporation. *Parker O-Ring Handbook*, 2021, www.parkerorings.com. Accessed: January 25, 2023.

(34) Bioenergy Technologies Office. *Sustainable Aviation Fuel: Review of Technical Pathways Report*, U.S. Department of Energy, 2020. <https://www.energy.gov/sites/default/files/2020/09/f78/beto-sust-aviation-fuel-sep-2020.pdf>.

(35) Gormley, R. J.; Link, D. D.; Baltrus, J. P.; Zandhuis, P. H. Interactions of jet fuels with nitrile o-rings: Petroleum-derived versus synthetic fuels. *Energy Fuels* **2009**, *23*, 857–861.

(36) Corporan, E.; Edwards, T.; Shafer, L.; DeWitt, M. J.; Klingshirn, C.; Zabarnick, S.; West, Z.; Striebich, R. C.; Graham, J. L.; Klein, J. Chemical, thermal stability, seal swell, and emissions studies of alternative jet fuels. *Energy Fuels* **2011**, *25*, 955–966.

(37) Boehm, R. C.; Yang, Z.; Heyne, J. Threshold Sooting Index of Sustainable Aviation Fuel Candidates from Composition Input Alone: Progress toward Uncertainty Quantification. *Energy Fuels* **2022**, *36*, 1916–1928.